Carbohydrate Polymers 192 (2018) 273–281

Contents lists available at ScienceDirect

Carbohydrate Polymers

journal homepage: www.elsevier.com/locate/carbpol

Distinct wall polymer deconstruction for high biomass digestibility under chemical pretreatment in *Miscanthus* and rice

Yuyang Li[a,b,1], Jingdi Zhuo[a,b,1], Peng Liu[a,b], Peng Chen[a,b], Huizhen Hu[a,b], Youmei Wang[a,b], Shiguang Zhou[a,b], Yuanyuan Tu[a,b], Liangcai Peng[a,b], Yanting Wang[a,b,*]

[a] Biomass and Bioenergy Research Centre, Huazhong Agricultural University, Wuhan 430070, China
[b] College of Plant Science and Technology, Huazhong Agricultural University, Wuhan, China

ARTICLE INFO

Keywords:
Wall polymers
Chemical pretreatment
Lignocellulose hydrolysis
Biomass saccharification
Glycan-directed antibodies
Immunolabeling

ABSTRACT

Miscanthus is a leading bioenergy crop and rice provides enormous biomass for biofuels. Using Calcofluor White staining, this work *in situ* observed an initial lignocellulose hydrolysis in two distinct *Miscanthus* accessions, rice cultivar (NPB), and *Osfc16* mutant after mild chemical pretreatments. In comparison, the *M. sin* and *Osfc16* respectively exhibited weak Calcofluor fluorescence compared to the *M. sac* and NPB during enzymatic hydrolysis, consistent with the high biomass saccharification detected *in vitro*. Using xyloglucan-directed monoclonal antibodies (mAbs), xyloglucan deconstruction was observed from initial cellulose hydrolysis, whereas the *M. sin* and *Osfc16* exhibited relatively strong immunolabeling using xylan-directed mAb, confirming previous findings of xylan positive impacts on biomass saccharification. Furthermore, the *M. sin* showed quick disappearance of RG-I immunolabeling with varied HG labelings between acid and alkali pretreatments. Hence, this study demonstrated a quick approach to explore wall polymer distinct deconstruction for enhanced biomass saccharification under chemical pretreatment in bioenergy crops.

1. Introduction

Plant cell walls represent enormous biomass resource for biofuels and chemical products (Cardona & Sanchez, 2007; Ragauskas et al., 2006). In principle, biomass conversion involves in three major steps: initial physical and chemical pretreatment of biomass for wall polymer deconstruction, sequential enzymatic hydrolysis of lignocellulose for fermentable sugar release, and final yeast fermentation of soluble sugars for bioethanol production (Carroll & Somerville, 2009; Wang et al., 2016). However, lignocellulose recalcitrance basically leads to an unacceptably expensive biomass process (Himmel et al., 2007; Xie & Peng, 2011), which is basically determined by plant cell wall composition, wall polymer feature and wall network style (Chen & Dixon, 2007; Li and Feng et al., 2014; Wang et al., 2016; Zahoor and Sun et al., 2017). Hence, it becomes important to sort out distinct deconstruction of major wall polymers for enhancing lignocellulose enzymatic hydrolysis upon various pretreatments in specific tissues and cell types in bioenergy crops.

Plant cell walls are comprised mainly of cellulose, hemicellulose and lignin with small amounts of pectin and wall proteins. In general, there are two major types of cell walls: a thinner pectin-rich primary cell wall and a thicker lignin-rich secondary cell wall (Somerville et al., 2004). Cellulose is composed of β-1,4-linked glucan chains that form crystalline microfibrils via hydrogen bonds, and cellulose crystallinity has been examined as the key negative factor on biomass enzymatic digestibility under various chemical pretreatments in different plant species (Laureano-Perez, Teymouri, Alizadeh, & Dale, 2005; Li et al., 2013; Li et al., 2015; Pei et al., 2016; Zhang et al., 2013). Hemicelluloses are a class of heterogeneous polysaccharides with distinct compositions including xyloglucan (XG), xylan, mannan and mixed-linkage glucan (Scheller & Ulvskov, 2010). As a major hemicellulosic component of secondary cell walls, xylan is reported as the positive factor on lignocellulose enzymatic saccharification by interaction with cellulose microfibrils via hydrogen bonds, leading to reduced cellulose crystallinity in grass plants examined (Ji, Zhang, Ling, Sun, & Xu, 2016; Jia et al., 2014; Li et al., 2013; Li et al., 2017; Zahoor and Sun et al., 2017). By comparison, xyloglucan is a major hemicellulosic constituent of primary cell walls, but little is known about their impacts on biomass

Abbreviations: mAbs, monoclonal antibodies; *M. sin*, *Miscanthus sinensis*; *M. sac*, *Miscanthus sacchariflorus*; XG, xyloglucan; HG, homogalacturonan; RG-I, rhamnogalacturonan-I

* Corresponding author at: Biomass and Bioenergy Research Centre, Huazhong Agricultural University, Wuhan 430070, China.
E-mail addresses: 707917973@qq.com (Y. Li), 479784828@qq.com (J. Zhuo), 752624417@qq.com (P. Liu), chenpeng@mail.hzau.edu.cn (P. Chen), jenny_8729@163.com (H. Hu), wym_quiet@yeah.net (Y. Wang), 124364692@qq.com (S. Zhou), yuant@mail.hzau.edu.cn (Y. Tu), lpeng@mail.hzau.edu.cn (L. Peng), wyt@mail.hzau.edu.cn (Y. Wang).
[1] Equal contribution author.

https://doi.org/10.1016/j.carbpol.2018.03.013
Received 16 December 2017; Received in revised form 2 February 2018; Accepted 8 March 2018
Available online 09 March 2018
0144-8617/

enzymatic saccharification (De Souza, Alvim Kamei, & Torres, 2015). Pectin is the most structurally complex polysaccharide in primary cell walls, and pectic polysaccharides mainly include homogalacturonan (HG), rhamnogalacturonan-I (RG-I) and rhamnogalacturonan-II. In particular, galacturonic acids are typical components of pectic polysaccharides (Atmodjo, Hao, & Mohnen, 2013). Despite of low level and complicated structure of pectin, recent reports have shown that pectin may play distinct roles in lignocellulose enzymatic hydrolysis, probably by negatively affecting cellulose crystallinity (De Souza et al., 2015; Wang, Huang, Li, Xiong, & Wang, 2015; Wang et al., 2016). However, much remains unknown about major pectic polysaccharides deconstruction and impacts on lignocellulose enzymatic hydrolysis under chemical pretreatments.

Chemical pretreatments have been broadly applied to extract wall polymers using alkali and acid agents such as KOH and H_2SO_4 (Singh, Suhag, & Dhaka, 2015; Wang et al., 2016). In general, alkali pretreatment could largely extract wall polymers by disassociating hydrogen bonds with cellulose microfibrils, whereas acid pretreatment mainly degrades wall polymers by splitting strong chemical bonds under high temperatures (Hendriks & Zeeman, 2009; Jin et al., 2016; Xu et al., 2012; Zahoor and Tu et al., 2017). Despite of distinct cell wall deconstruction between alkali and acid pretreatments, it remains interesting to *in situ* observe characteristic dissociation and deconstruction of each wall polymer at specific cells and tissues of plants.

Recently, a large set of plant glycan-directed monoclonal antibodies (mAbs) have been used as probes to visualize the localization of glycan epitope (Avci, Pattathil, & Hahn, 2012; Moller et al., 2007; Pattathil et al., 2010). This technique is also applied to study the distribution patterns of glycan epitopes in plant cell walls after hydrothermal pretreatments (Demartini et al., 2011). However, this technology has not been applied to *in situ* observe time-course wall polymer deconstruction during enzymatic hydrolysis after chemical pretreatments in rice and *Miscanthus* bioenergy crops. In this study, we presented the immunolabeling images of major wall polysaccharides epitopes during time course of lignocellulose enzymatic hydrolysis after mild acid or alkali pretreatments of stem tissues in two representative *Miscanthus* accessions and two rice (*Oryza sativa L*) samples by using four specific glycan-directed mAbs. Meanwhile, we *in situ* observed cellulose enzymatic digestions using Calcofluor White staining with cellulose microfibrils, and detected biomass enzymatic saccharification by quantitatively measuring hexoses yields released from enzymatic hydrolysis after chemical pretreatments *in vitro*. Notably, this study also performed chemical analysis of major monosaccharides during the time-course enzymatic hydrolysis, which confirmed the *in situ* observations of the immunolabeling of major wall polysaccharides epitopes. Hence, this study demonstrated a quick approach to observe wall polymer distinct deconstruction for enhanced biomass enzymatic saccharification under chemical pretreatments.

2. Materials and methods

2.1. Sample collection

Miscanthus sinensis (*M. sin*), *Miscanthus sacchariflorus* (*M. sac*), rice cultivar (Nipponbare, NPB) and rice *Osfc16* mutant (Li et al., 2017) were collected in the experimental fields of Huazhong Agricultural University, Wuhan, China. The top 11th internode stems of *Miscanthus* and the upper second internode stems of rice were respectively collected: (1) 8 μm thick sections embedded in paraplast plus boxes for immunolabeling and (2) 100 μm thick sections used for chemical analyses of sugars.

2.2. Sample preparation for immunolabeling

Internode stem samples were cut into 0.5–1.0 cm pieces and fixed in 70% (v/v) ethanol, 5% (v/v) formaldehyde and 5% (v/v) glacial acetic acid, and then dehydrated by ethanol and xylene series. The xylene solution was gradually replaced by paraplast plus (Sigma, USA) chips at 60 °C, and the samples were transferred to 100% wax (24 h, 37 °C), placed in sample moulds filled with molten wax and left at room temperature to solidify (for at least 12 h). The stems were sectioned into 8 μm slices, mounted on polysine coated microscope slides and dried for three days at 37 °C. Sections were de-waxed with xylene and rehydrated through an ethanol series from 100% to 0%. Sections were washed extensively in PBS Buffer. Two independent biological replicates were performed for each sample.

2.3. Immunolabeling

Three glycan-directed mAbs (CCRC-M99, CCRC-M147, CCRC-M35) were prepared from 5-fold dilution of hybridoma cell culture supernatant, and one glycan-directed mAb (JIM5) was from a 10-fold dilution using 3% MP/PBS buffer as previously described by Avci et al. (2012). The stem section samples were incubated in PBS containing 5% (w/v) milk protein (MP/PBS) and a diluted antibody solution for 1.5 h. Samples were then washed with PBS at least 3 times and incubated with a 200-fold diluted secondary antibody (Alexa Fluor 488 anti-mouse IgG, Invitrogen, A11001 for CCRC antibodies; Alexa Fluor 488 anti-rat IgG, Invitrogen, A-11006 for JIM antibody) linked to fluorescein isothiocyanate (FITC) in PBS for 1.5 h in darkness.

2.4. Calcofluor White staining

For cellulose staining, the stem section samples were washed in PBS at least 3 times and incubated with Calcofluor White (0.25 μg/mL; Fluorescent Brightner 28, Sigma, UK) for 5 min in darkness and then washed three times with PBS at room temperature (Cao et al., 2014).

2.5. Fluorescence imaging

Fluorescence was observed with a microscope equipped with epifluorescence irradiation and DIC optics (Olympus BX-61). Fluorescence images generated with Calcofluor White staining (blue) and immunofluorescence (green) were observed. Images were captured with a Hamamatsu ORCA285 camera and Improvision Velocity software. All micrographs were captured using equivalent settings, and relevant micrographs were processed in equivalent ways for generation of datasets.

2.6. Pretreatment and enzymatic hydrolysis

Stem sections were pretreated with 0.5 M KOH (rice) and 1 M KOH (*Miscanthus*) at 25 °C for 2 h, or with 1% H_2SO_4 at 70 °C (rice) and 1% H_2SO_4 at 100 °C (*Miscanthus*) for 1 h. The pretreated samples were washed three times with distilled water until pH7.0, and the pellets were then incubated with 1.6 g/L mixed cellulases (containing β-glucanase ≥ 2.98×10^4 U, cellulase ≥ 298 U and xylanase ≥ 4.8×10^4 U, purchased from Imperial Jade Bio-technology Co., Ltd., China) for 0.5 h, 1 h, 2 h (rice), or 2 h, 4 h, 12 h, 24 h (*Miscanthus*), respectively. After washing three times with the enzymatic digested samples, all supernatants were collected for chemical analysis of total hexoses, pentoses and uronic acids. All samples were conducted in biological triplicate.

2.7. Colorimetric assay of hexoses, pentoses and uronic acids

The UV–VIS spectrometer (V-1100D, Shanghai MAPADA Instruments Co., Ltd. Shanghai, China) was used for the absorbance reading. Hexoses were detected using the anthrone/H_2SO_4 method (Fry, 1988), and pentoses were tested using the orcinol/HCl method (Huang et al., 2012). The standard curves for hexoses and pentoses were drawn using D-glucose and D-xylose as standards (purchased from

Sinopharm Chemical Reagent Co., Ltd.) respectively. Because high pentose levels can affect the absorbance reading at 620 nm for hexose assay, deduction from the pentose reading at 660 nm was carried out for final hexose calculation. A series of xylose concentrations were analyzed for plotting the standard curve referred to for the deduction, which was verified by gas chromatography–mass spectrometry (GC–MS) analysis. Total uronic acids were assayed using *m*-hydroxybiphenyl/NaOH method (Fry, 1988). All experiments were performed in biological triplicate.

2.8. Monosaccharide determination by GC–MS

Monosaccharides were determined by GC–MS as previously described by Li et al. (2013). GC–MS analysis was performed based on analytical conditions: Restek Rxi–5 ms, 30 m × 0.25 mm ID × 0.25 um df column; carrier gas: helium; injection method: split; split ratio: 20:1; injection port: 250 °C; interface: 250 °C; injection volume: 1.0 uL; temperature program: from 155 °C (held for 23 min) to 200 °C (held for 5 min) at 3.8 °C/minute, then from 200 °C to 300 °C (held for 2 min) at 20 °C/minute; ion Source: E1; ion source temperature: 200 °C; ACQ mode: SIM. Mass spectra were acquired with full scans based on the temperature program from 50 to 500 *m/z* in 0.45 s. Calibration curves of all analytes routinely yielded correlation coefficients of 0.999 or higher.

3. Results

3.1. Observation of cellulose hydrolysis upon alkali pretreatment in situ

In the present study, cellulose hydrolysis was *in situ* characterized in *Miscanthus* and rice samples using Calcofluor White staining with stem sections after KOH pretreatment at 25 °C for 2 h (Fig. 1). Under mild alkali pretreatments, *Miscanthus* and rice samples exhibited Calcofluor White, similar to their controls (without pretreatment). However, treated with mixed-cellulases for 2 h enzymatic hydrolysis, two *Miscanthus* accessions started to show reduced Calcofluor white fluorescence in parenchyma, and after 24 h enzymatic hydrolysis, the fluorescence was observed in partial vascular bundles (Fig. 1a). By comparison, the fluorescence disappeared in the *M. sin* accession earlier than that of *M. sac* accession in parenchyma during the time-course enzymatic hydrolysis. Because parenchyma and vascular bundles are respectively rich in primary and secondary cell walls (Keegstra, 2010; Somerville et al., 2004), these observations indicated that primary wall cellulose is initially digested by the mixed-cellulases. While treated with mixed-cellulases for 0.5 h, rice cultivar (NPB) and *Osfc16* mutant (Li et al., 2017) only showed fluorescence in vascular bundles, and the fluorescence declined during the time-course enzymatic hydrolysis, in particular in the *Osfc16* mutant (Fig. 1b). Further incubation with mixed-cellulases, the stem tissues of rice were destructed (data not shown), probably due to much cellulose digestion and wall polysaccharide deconstruction.

3.2. Wall polymers deconstruction during cellulose hydrolysis after KOH pretreatment

To detect major non-cellulosic polysaccharides *in situ* during cellulose enzymatic hydrolysis, we employed four representative mAbs to show the polysaccharides epitopes in *Miscanthus* and rice samples. The results shown in Fig. 2 indicated the strong recognition of XG in the phloem regions of *Miscanthus* and rice samples, and the immunolabeling was slightly changed from KOH pretreatments (Fig. 2a, e). However, the XG epitopes were immediately lost from initial enzymatic hydrolysis in *Miscanthus* (2 h) and rice (0.5 h), indicating that XG epitopes could be efficiently deconstructed by cellulose enzymatic hydrolysis in all biomass samples.

Miscanthus and rice samples showed significantly different fluorescence patterns binding to the xylan-directed mAbs CCRC-M147 during enzymatic hydrolysis after alkali pretreatment (Fig. 2b, f). Despite of broad immunolabeling distribution in vascular bundles in two *Miscanthus* accessions, the labeling was gradually declined in the wall polysaccharides epitopes recognized by the selected mAbs after KOH pretreatment (defined as 0 h) and sequential enzymatic hydrolysis, and the recognition was not detected from 12 h (*M. sac*) or 24 h (*M. sin*) incubation with mixed-cellulases (Fig. 2b). By comparison, rice samples showed strong recognition with whole stem sections after alkali pretreatment (Fig. 2f), probably due to the increased access to xylan epitopes after alkali pretreatment. Notably, after 0.5 h enzymatic hydrolysis, rice samples exhibited strong immunolabeling in entire parenchyma, and the epitopes were hardly observed after 2 h enzymatic hydrolysis. Because the mixed-cellulases contain xylanase with high activity, the immunolabeling should be derived from the partially-undigested xylan that was associated with cellulose and/or other wall polymers. In addition, *Osfc16* mutant exhibited relatively stronger immunolabeling than those of NPB cultivar, consistent with the previous findings about high xylans level in the mutant (Li et al., 2017).

Because HG is the most abundant pectic polysaccharides, this study examined distribution of partially methyl-esterified HG recognized by JIM5. In *Miscanthus* accessions, pectic related epitopes were observed in the phloem, xylem and intercellular spaces, and the immunolabeling was declined slightly after alkali pretreatment (Fig. 2c). However, the immunolabeling epitopes were not observed after sequential enzymatic hydrolysis for 2 h and 4 h in *M. sac* and *M. sin*, respectively. By comparison, the labeling was reduced considerably by the alkali pretreatment in rice samples and was lost after 0.5 h enzymatic hydrolysis (Fig. 2g). Meanwhile, using CCRC-M35 to bind RG-I backbone, the immunolabling of RG-I epitopes was mainly observed in the intercellular spaces, and reduced after alkali pretreatment (Fig. 2d, h). Because the mixed-cellulases do not have activity of pectic polysaccharides degradation, the results suggested that pectin should be rapidly deconstructed with cellulose or hemicelluose during enzymatic hydrolysis in both *Miscanthus* and rice samples.

3.3. Enhanced biomass saccharification in M. sin and Osfc16 under alkali pretreatment

In this study, biomass enzymatic saccharification was measured by calculating hexoses and pentoses (xylose and arabinose) yields released from commercial mixed-cellulases enzymatic hydrolysis after chemical pretreatments using stem sections of *Miscanthus* and rice samples (Fig. 3). As a result, alkali pretreatment mainly released pentoses and uronic acids, with extremely low level of hexoses. However, the sequential enzymatic hydrolysis released large amounts of hexoses (glucose) and pentoses in both *Miscanthus* and rice samples. Notably, during time course of enzymatic hydrolysis, *M. sin* accession showed significantly higher hexoses yields than those of *M. sac* accession at $P < 0.05$ and $P < 0.01$ levels (n = 3) (Fig. 3a, b), consistent with relatively less Calcofluor White fluorescence at *M. sin* sections (Fig. 1a). Similarly, *Osfc16* mutant also exhibited significantly higher hexoses (glucose) yield than that of NPB cultivar after 2 h enzymatic hydrolysis (Fig. 3c, d), in supporting of previous findings about significantly higher hexoses yield in the *Osfc16* mutant (Li et al., 2017). Therefore, these results suggested that Calcofluor White staining could not only be used to detect lignocellulose enzymatic hydrolysis *in situ*, but it may also be applicable for predicting biomass saccharification *in vitro*.

3.4. Acid pretreatment for wall polymer deconstruction and biomass saccharification

To compare with the alkali pretreatment, this study also performed acid pretreatment of transverse sections of *Miscanthus* and rice stems. Because rice stem section was rapidly deconstructed by 1% H_2SO_4 at 100 °C, this study conducted the acid pretreatment at 70 °C for 1 h, but

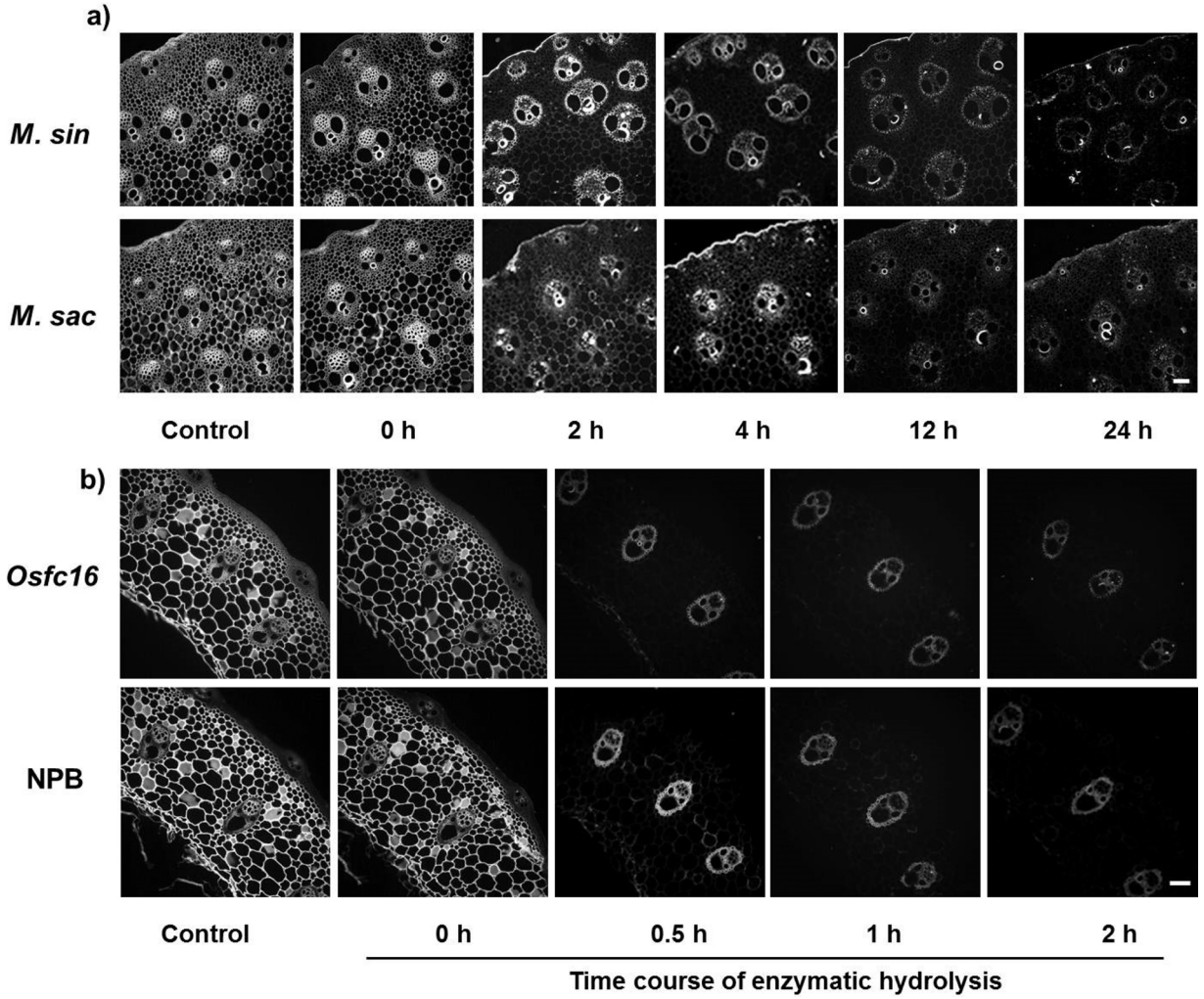

Fig. 1. Calcofluor White staining in transverse sections of *Miscanthus* and rice stems from alkali pretreatment (0 h) and subsequent time course of enzymatic hydrolysis. (a) Two *Miscanthus* accessions (*M. sin*, *M. sac*); (b) rice mutant (*Osfc16*) and cultivar (NPB); Scale bar = 100 μm.

it remained to use 100 °C for *Miscanthus* samples. After acid pretreatment, two *Miscanthus* accessions exhibited similar Calcofluor White fluorescence patterns during enzymatic hydrolysis (Fig. 4a) as observed of the alkali pretreatment (Fig. 1a). Accordingly, the acid pretreatment could lead to similar hexoses (glucose) yields released from enzymatic hydrolysis in *Miscanthus* accessions, compared with the alkali pretreatment, but it remained significantly higher hexoses yield in *M. sin* than in *M. sac* (Figs. Fig. S1; 3a, b). By comparison, rice samples were deconstructed from 0.5 h enzymatic hydrolysis after acid pretreatment, but the Calcofluor White fluorescence was observed in partial parenchyma, even though enzymatic hydrolysis for 2 h (Fig. 4b), which was different from alkali pretreatment and sequential enzymatic hydrolysis (Fig. 1b). In addition, the *Osfc16* mutant had significantly higher hexoses yields than those of NPB cultivar (Figs. Fig. S1; 3c, d), consistent with relatively weak fluorescence in the mutant during enzymatic hydrolysis (Fig. 4b).

Furthermore, this study also observed epitopes of xyloglucan, xylan and pectin during enzymatic hydrolysis after acid pretreatment in stem sections using four mAbs (Fig. 5). As previously observed from alkali pretreatment, two *Miscanthus* accessions showed quick digestion of XG by enzymatic hydrolysis for 2 h after acid pretreatment (Fig. 5a). However, the rice samples exhibited a complete XG deconstruction by acid pretreatment prior to enzymatic hydrolysis (Fig. 5e), different from alkali pretreatments (Fig. 2e). Compared with observations from alkali pretreatments (Fig. 2b, f), the xylan epitope recognized by CCRC-M147 was not detected in two *Miscanthus* accessions after acid pretreatments and sequential 2 h enzymatic hydrolysis (Fig. 5b), whereas the immunolabeling remained observed after alkali pretreatments and 12 h enzymatic hydrolysis (Fig. 2b). Despite that rice samples exhibited relatively weak immunolabeling in vascular bundles by enzymatic hydrolysis after acid pretreatments, they did not show any dot-labeling that had been observed in the alkali pretreatment. (Fig. 5f, f).

With respect to HG and RG-I related epitopes, *Miscanthus* and rice samples showed distinct immunolabeling patterns after acid pretreatments (Fig. 5c, d, g, h), compared with alkali pretreatments (Fig. 2c, d, g, h). In general, the immunolabeling was quickly declined during enzymatic hydrolysis after acid pretreatments. Exceptionally, the RG-I epitopes were not detected from 2 h enzymatic hydrolysis in *M. sin* accession (Fig. 5d), which may partially cause its relatively higher hexoses (glucose) yields than those of *M sac*. In addition, *M. sin* accession had relatively higher pentoses and uronic acids yields than those of *M. sac* accession, whereas *Osfc16* mutant remained higher pentoses and uronic acids than those of NPB cultivar, consistent with their distinct hexoses yields released from enzymatic hydrolysis after acid pretreatments (Fig. S1).

3.5. Direct cellulose enzymatic hydrolysis for wall polymer deconstruction

Without any pretreatment, this study also observed wall polymer deconstruction and biomass saccharification from direct enzymatic

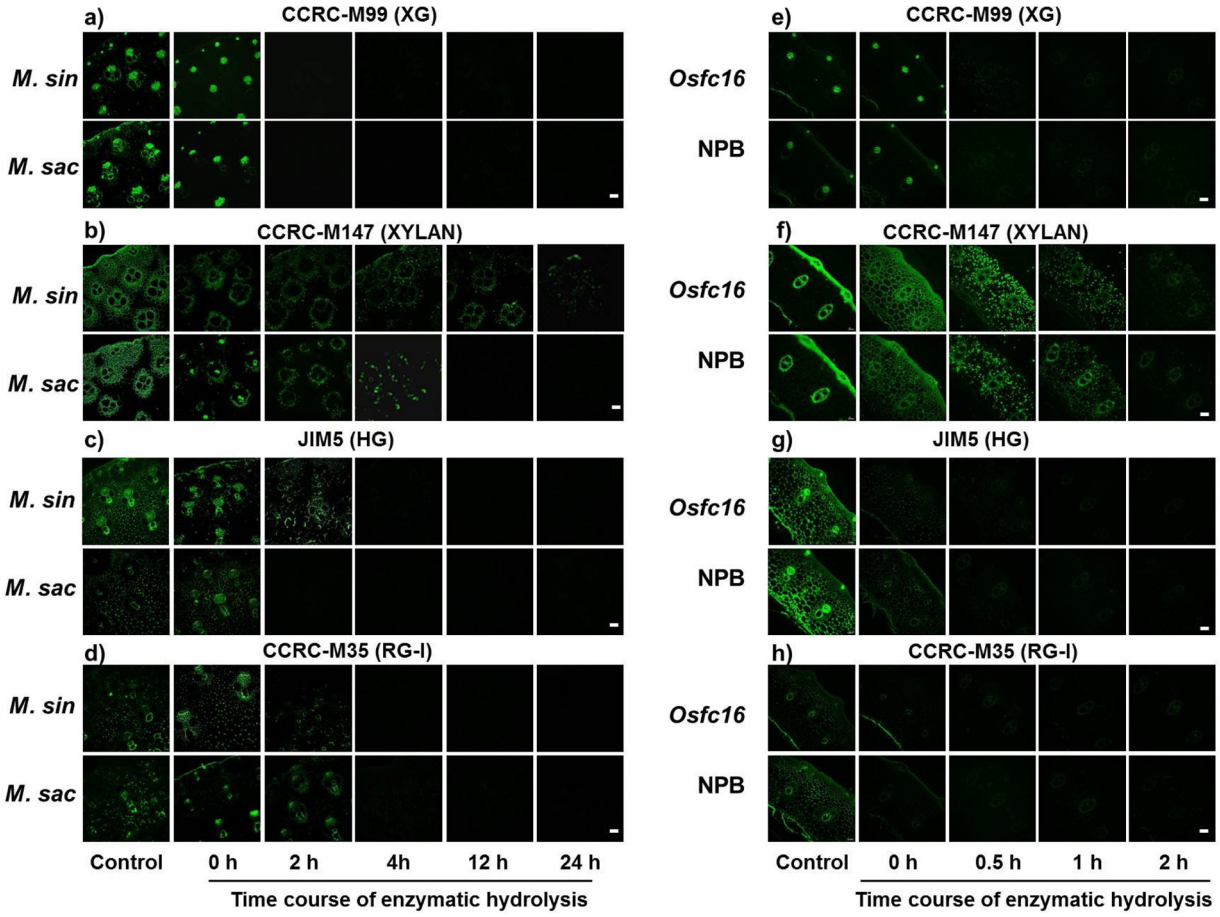

Fig. 2. Immunolocalization of hemicellulosic and pectic polysaccharides epitopes in transverse sections of *Miscanthus* and rice stems from alkali pretreatment (0 h) and subsequent time course of enzymatic hydrolysis. (a-d) Two *Miscanthus* accessions (*M. sin*, *M. sac*); (e–h) rice mutant (*Osfc16*) and cultivar (NPB); Scale bar = 100 μm.

hydrolysis using stem sections of *Miscanthus* and rice samples. Compared with the alkali and acid pretreatments (Figs. 1 and 4), both *Miscanthus* and rice samples showed stronger Calcofluor White fluorescence during direct enzymatic hydrolysis (Fig. 6), consistent with their lower hexoses (glucose) yields released from direct enzymatic hydrolysis (Fig. S2). By comparison, the Calcofluor White fluorescence was not observed in parenchyma from direct enzymatic hydrolysis in *M. sin* accession, but remained in partial parenchyma of *M. sac* accession (Fig. 6a), which was consistent with significantly higher biomass saccharification (hexoses/glucose yields) in *M. sin* accession (Fig. S2). By contrast, rice samples exhibited Calcofluor White fluorescence in almost whole stem sections, and *Osfc16* mutant showed relatively weaker

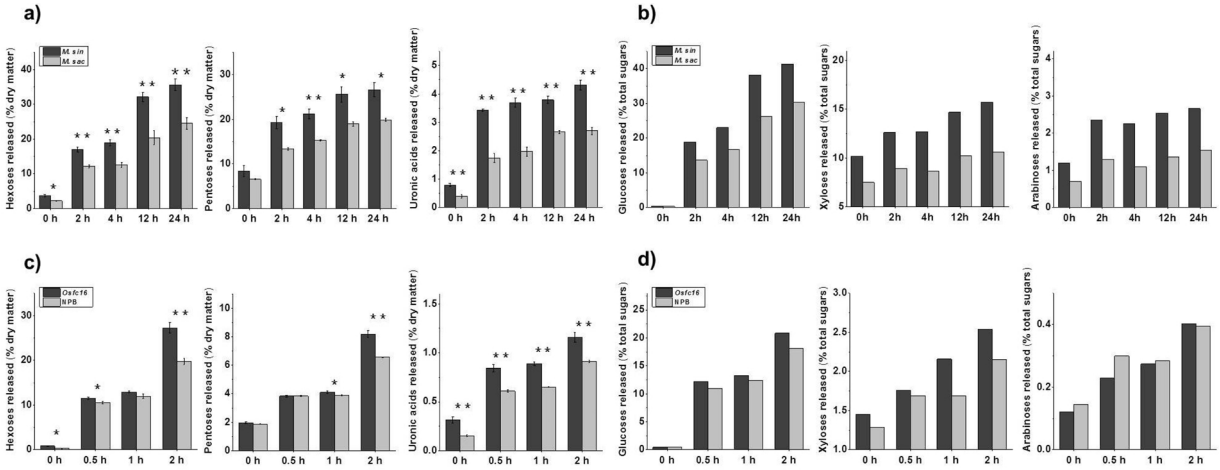

Fig. 3. Sugars yields released from alkali pretreatment (0 h) and subsequent time course of enzymatic hydrolysis in transverse sections of *Miscanthus* and rice stems. (a, c) Three sugars yields (hexoses, pentoses, uronic acids), the bar as mean ± SD (n = 3); (b, d) Percentage of glucose, xylose and arabinose (% of total sugars); * and ** Indicated significant difference by *t*-test at $P < 0.05$ and 0.01 levels between two *Miscanthus* accessions (*M. sin*, *M. sac*), or between rice mutant (*Osfc16*) and cultivar (NPB).

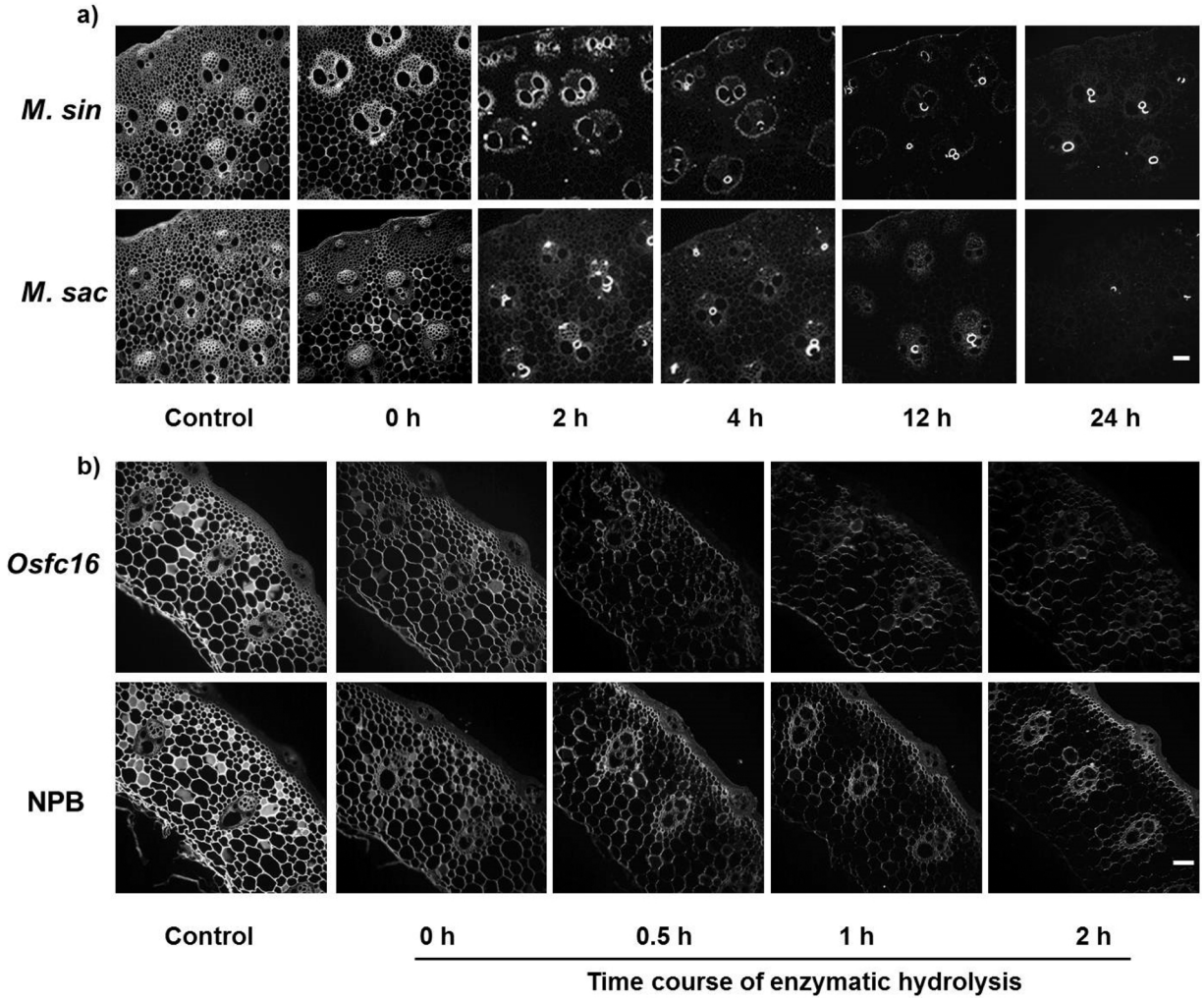

Fig. 4. Calcofluor White staining in transverse sections of *Miscanthus* and rice stems from acid pretreatment (0 h) and subsequent time course of enzymatic hydrolysis. (a) Two *Miscanthus* accessions (*M. sin* and *M. sac*); (b) rice mutant (*Osfc16*) and cultivar (NPB); Scale bar = 100 μm.

fluorescence than that of NPB cultivar after direct enzymatic hydrolysis for 1 h and 2 h (Fig. 6b), consistent with significantly higher biomass saccharification in *Osfc16* mutant (Fig. S2).

In terms of the immunolabeling epitopes of four non-cellulosic polysaccharides deconstruction during direct enzymatic hydrolysis, *Miscanthus* and rice samples did not show much reduced immunolabeling of xylan, HG and RG-I epitopes (Fig. S3). Compared with the enzymatic hydrolysis after chemical pretreatment (Figs. 3; Fig. S2), direct enzymatic hydrolysis leaded to relatively low pentoses and uronic acids yields (Fig. S2). However, the immunolabeling of XG epitopes was not detected after direct enzymatic hydrolysis in *Miscanthus* and rice samples (Fig. S3). Hence, direct enzymatic hydrolysis could mainly digest cellulose and xyloglucan with little impacts on other non-cellulosic polysaccharide deconstruction.

4. Discussion

Miscanthus has been considered as a leading bioenergy crop, and rice (*Oryza sativa L*) is a major food crop around world with large biomass residues for biofuels. Over the past years, attempts have been made to select desirable *Miscanthus* accessions and rice transgenic lines that are of high biomass saccharification and reduced lignocellulose recalcitrance (Li et al., 2013; Li et al., 2017; Li and Si et al., 2014; Sun et al., 2017; Zhang et al., 2013; Zhang et al., 2016). Although *M. sin* accession and rice *Osfc16* mutant have much higher biomass saccharification than those of *M. sac* and NPB cultivar (Huang et al., 2012; Li et al., 2016; Li et al., 2017), this study explored their distinct cellulose enzymatic hydrolysis *in situ* at plant tissue and cell levels using Calcofluor White staining. Because Calcofluor White staining is a useful approach, it should be applicable for predicting biomass enzymatic saccharification in bioenergy crops. Importantly, this study well demonstrated that primary wall-rich cellulose in parenchyma could be efficiently digested by initial enzymatic hydrolysis. It has also suggested that specific modification of secondary cell walls in vascular bundles may lead to largely enhanced cellulose hydrolysis in bioenergy crops. Accordingly, optimal pretreatment technology should be considered to target for vascular bundles deconstruction.

More recently, integrative analyses have been performed to find out the major wall polymer features that distinctively affect biomass saccharification using large populations of *Miscanthus* accessions and rice mutants (Li et al., 2013; Li et al., 2015; Sun et al., 2017). As the major hemicellulose of secondary cell walls in grasses, xylan has been examined to positively affect biomass saccharification by reducing cellulose crystallinity in *Miscanthus* and rice samples (Wang et al., 2016). Hence, this study confirmed xylan positive roles in biomass saccharification *in situ*, due to *M. sin* accession and *Osfc16* mutant showing relatively strong immunolabeling of xylan epitopes than those of *M. sacchariflorus* accession and NPB cultivar during time course of enzymatic hydrolysis after alkali pretreatments. We interpreted that those remaining labeling should be derived from partially-undigested xylan

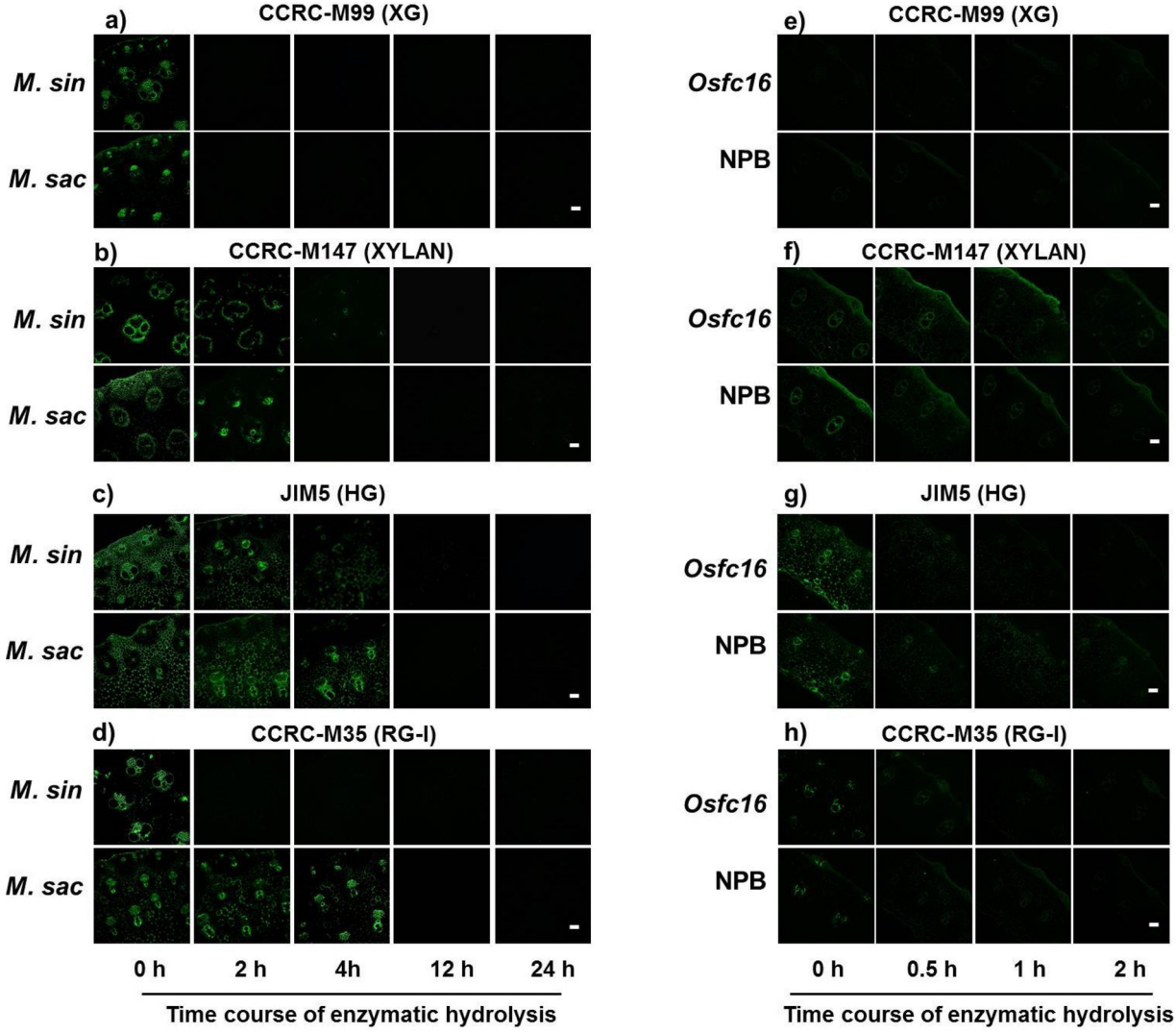

Fig. 5. Immunolocalization of hemicellulosic and pectic polysaccharides epitopes in transverse sections of *Miscanthus* and rice stems from acid pretreatment (0 h) and subsequent time course of enzymatic hydrolysis. (a-d) Two *Miscanthus* accessions (*M. sin* and *M. sac*); (e–h) rice mutant (*Osfc16*) and cultivar (NPB); Scale bar = 100 μm.

that are associated with cellulose microfibrils and/or other wall polymers, which may not only allow cellulases enzyme accessible to cellulose surface, but may also maintain cellulose microfibrils at native state with low crystallinity for an efficient cellulose hydrolysis. Hence, despite glycan-directed immuolabelling technology has been broadly applied to observe major wall polysaccharide distribution *in situ* in different plant species (Da Costa et al., 2017; Pattathil, Avci, Zhang, Cardenas, & Hahn, 2015; Peralta, Venkatachalam, Stone, & Pattathil, 2017), this study could provide a useful approach to explore major wall polymer roles in biomass enzymatic hydrolysis of bioenergy crops in the future.

Furthermore, this study well examined that xyloglucan could be efficiently digested from initial enzymatic hydrolysis, no matter chemical pretreatment is performed or not, suggesting that xyloglucan may have little impact on lignocellulose enzymatic digestion. As xyloglucan contains β-1,4-glucan backbone, genetic overexpression of xyloglucan gene may lead to largely enhanced saccharification efficiency in bioenergy crops, which should be an applicable approach for wall modification in the bioenergy crops.

Because this study has found that pectic polysaccharides were deconstructed from initial cellulose enzymatic hydrolysis after alkali pretreatment in *Miscanthus* accessions and also could be directly removed by alkali pretreatment in rice samples, it suggested that HG and RG-I should not much affect biomass enzymatic saccharification upon alkali pretreatment. However, both HG and RG-I may be the factors affecting biomass digestibility from acid pretreatments distinctive in two *Miscanthus* accessions. For instance, compared with *M. sac* accession, *M. sin* exhibited a quicker deconstruction of RG-I epitopes and relatively less immunolabeling of HG epitopes from enzymatic hydrolysis after acid pretreatment (Fig. 5c, d), which may partially cause significantly higher hexoses (glucose) yields in the *M. sinensis* accession. Surprisingly, although the hexoses (glucose) yields remained rising from the time course of direct enzymatic hydrolysis without any pretreatment, the immunolabeling of HG and RG-I epitopes was not much altered in *Miscanthus* and rice samples (Fig. S3), indicating that both pectic polysaccharides may be tightly associated with other non-cellulosic polymers in wall networks. Therefore, this study also suggested that specific pretreatment technology may be powerful to sort out wall polysaccharide distinct roles in biomass enzymatic saccharification. In addition, typical genetic mutants and transgenic lines should be used to *in situ* explore wall polysaccharide deconstruction for biomass saccharification in the future.

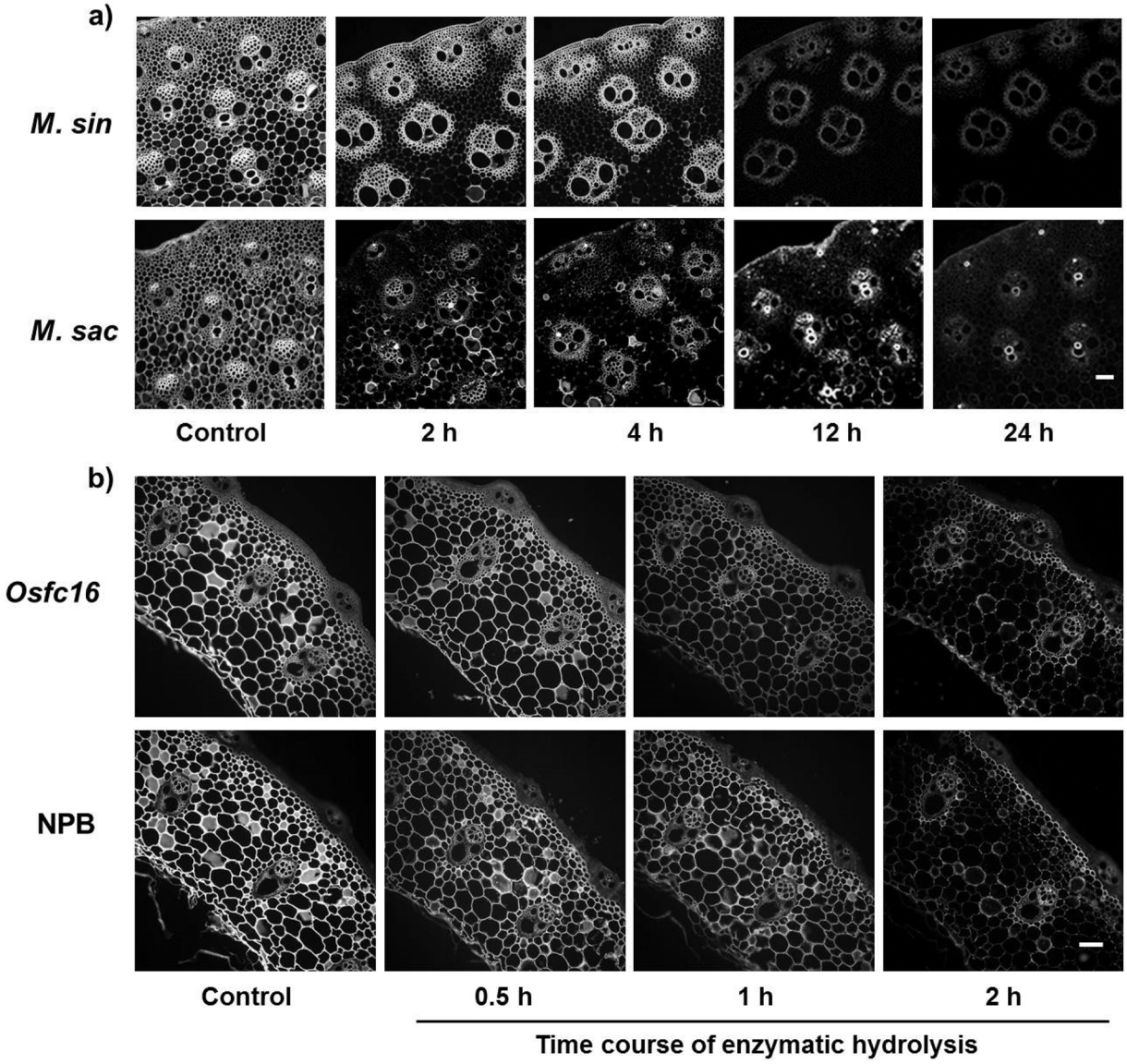

Fig. 6. Calcofluor White staining in transverse sections of *Miscanthus* and rice stems during time course of enzymatic hydrolysis without pretreatment. (a) Two *Miscanthus* accessions (*M. sin*, *M. sac*); (b) rice mutant (*Osfc16*) and cultivar (NPB); Scale bar = 100 μm.

5. Conclusion

This study *in situ* detected an efficient and quick cellulose hydrolysis in primary wall-rich cells and tissues in *Miscanthu* and rice samples. Using immunolabling of glycan epitopes, it also examined a distinct deconstruction of four major wall polysaccharides (xyloglucan, xylan, HG, and RG-I) during the time course of mixed-cellulases enzymatic hydrolysis upon alkali or acid pretreatments, which interpreted why *M. sin* accession and rice *Osfc16* mutant have significantly higher biomass saccharification *in vitro*. Hence, this study provides a quick approach to dynamically explore wall polysaccharide distinct deconstruction for enhanced biomass enzymatic saccharification in bioenergy crops.

Acknowledgements

This work was supported in part by grants from the National Science Foundation of China (31670296), Fundamental Research Funds for the Central Universities of China (2662015PY018) and the National 111 Project (B08032). Generation of the CCRC-series of monoclonal antibodies used in this work was supported by a grant from the NSF Plant Genome Program (DBI-0421683), and distribution of the JIM and MAC antibodies used in this work was supported in part by NSF grants (DBI-0421683 and RCN 009281).

Appendix A. Supplementary data

Supplementary data associated with this article can be found, in the online version, at https://doi.org/10.1016/j.carbpol.2018.03.013.

References

Atmodjo, M. A., Hao, Z., & Mohnen, D. (2013). Evolving views of pectin biosynthesis. *Annual Review of Plant Biology, 64*, 747–779.
Avci, U., Pattathil, S., & Hahn, M. G. (2012). Immunological approaches to plant cell wall and biomass characterization: Immunolocalization of glycan epitopes. *Methods in Molecular Biology, 908*, 73–82.
Cao, Y., Li, J., Yu, L., Chai, G., He, G., Hu, R., et al. (2014). Cell wall polysaccharide distribution in *Miscanthus lutarioriparius* stem using immuno-detection. *Plant Cell Reports, 33*(4), 643–653.
Cardona, C. A., & Sanchez, O. J. (2007). Fuel ethanol production: Process design trends and integration opportunities. *Bioresource Technology, 98*(12), 2415–2457.
Carroll, A., & Somerville, C. (2009). Cellulosic biofuels. *Annual Review of Plant Biology, 60*, 165–182.
Chen, F., & Dixon, R. A. (2007). Lignin modification improves fermentable sugar yields for biofuel production. *Nature Biotechnology, 25*(7), 759–761.

Da Costa, R. M. F., Pattathil, S., Avci, U., Lee, S. J., Hazen, S. P., Winters, A., et al. (2017). A cell wall reference profile for *Miscanthus* bioenergy-crops highlights compositional and structural variations associated with development and organ origin. *New Phytologist, 213*(4), 1710–1725.

De Souza, A. P., Alvim Kamei, C. L., Torres, A. F., et al. (2015). How cell wall complexity influences saccharification efficiency in *Miscanthus sinensis*. *Journal of Experimental Botany, 66*(14), 4351–4365.

Demartini, J. D., Pattathil, S., Avci, U., Szekalski, K., Mazumder, K., Hahn, et al. (2011). Application of monoclonal antibodies to investigate plant cell wall deconstruction for biofuels production. *Energy & Environmental Science, 4*, 4332.

Fry, S. C. (1988). *The growing plant cell wall. Chemical and metabolic analysis*. London: Longman95–97.

Hendriks, A. T., & Zeeman, G. (2009). Pretreatments to enhance the digestibility of lignocellulosic biomass. *Bioresource Technology, 100*(1), 10–18.

Himmel, M. E., Ding, S. Y., Johnson, D. K., Adney, W. S., Nimlos, M. R., Brady, et al. (2007). Biomass recalcitrance: Engineering plants and enzymes for biofuels production. *Science, 315*(5813), 804–807.

Huang, J., Xia, T., Li, A., Yu, B., Li, Q., Tu, Y., et al. (2012). A rapid and consistent near infrared spectroscopic assay for biomass enzymatic digestibility upon various physical and chemical pretreatments in *Miscanthus*. *Bioresource Technology, 121*, 274–281.

Ji, Z., Zhang, X., Ling, Z., Sun, R., & Xu, F. (2016). Tissue specific response of Miscanthus × giganteus to dilute acid pretreatment for enhancing cellulose digestibility. *Carbohydrate Polymers, 154*, 247–256.

Jia, J., Yu, B., Wu, L., Wang, H., Wu, Z., Li, M., et al. (2014). Biomass enzymatic saccharification is determined by the non-KOH-extractable wall polymer features that predominately affect cellulose crystallinity in corn. *PUBLIC LIBRARY OF SCIENCE, 9*(9), e108449.

Jin, W., Chen, L., Hu, M., Sun, D., Li, A., Li, Y., et al. (2016). Tween-80 is effective for enhancing steam-exploded biomass enzymatic saccharification and ethanol production by specifically lessening cellulase absorption with lignin in common reed. *Applied Energy, 175*, 82–90.

Keegstra, K. (2010). Plant cell walls. *Plant Physiology, 154*(2), 483–486.

Laureano-Perez, L., Teymouri, F., Alizadeh, H., & Dale, B. E. (2005). Understanding factors that limit enzymatic hydrolysis of biomass characterization of pretreated corn strover. *Applied Biochemistry and Biotechnology, 121–124*, 1081–1099.

Li, M., Feng, S., Wu, L., Li, Y., Fan, C., Zhang, R., et al. (2014). Sugar-rich sweet sorghum is distinctively affected by wall polymer features for biomass digestibility and ethanol fermentation in bagasse. *Bioresource Technology, 167*, 14–23.

Li, M., Si, S., Hao, B., Zha, Y., Wan, C., Hong, S., et al. (2014). Mild alkali-pretreatment effectively extracts guaiacyl-rich lignin for high lignocellulose digestibility coupled with largely diminishing yeast fermentation inhibitors in Miscanthus. *Bioresource Technology, 169*, 447–454.

Li, F., Ren, S., Zhang, W., Xu, Z., Xie, G., Chen, Y., et al. (2013). Arabinose substitution degree in xylan positively affects lignocellulose enzymatic digestibility after various NaOH/H_2SO_4 pretreatments in *Miscanthus*. *Bioresource Technology, 130*, 629–637.

Li, F., Zhang, M., Guo, K., Hu, Z., Zhang, R., Feng, Y., et al. (2015). High-level hemicellulosic arabinose predominately affects lignocellulose crystallinity for genetically enhancing both plant lodging resistance and biomass enzymatic digestibility in rice mutants. *Plant Biotechnology Journal, 13*, 514–525.

Li, X., Liao, H., Fan, C., Hu, H., Li, Y., & Li, J. (2016). Distinct geographical distribution of the *Miscanthus* accessions with varied biomass enzymatic saccharification. *PUBLIC LIBRARY OF SCIENCE, 11*, e0160026.

Li, F., Xie, G., Huang, J., Zhang, R., Li, Y., Zhang, M., et al. (2017). *OsCESA9* conserved-site mutation leads to largely enhanced plant lodging resistance and biomass enzymatic saccharification by reducing cellulose DP and crystallinity in rice. *Plant Biotechnology Journal, 15*(9), 1093–1104.

Moller, I., Sørensen, I., Bernal, A. J., Blaukopf, C., Lee, K., Øbro, J., et al. (2007). High-throughput mapping of cell-wall polymers within and between plants using novel microarrays. *The Plant Journal, 50*(6), 1118–1128.

Pattathil, S., Avci, U., Baldwin, D., Swennes, A. G., McGill, J. A., Popper, Z., et al. (2010). A comprehensive toolkit of plant cell wall glycan-directed monoclonal antibodies. *Plant Physiology, 153*(2), 514–525.

Pattathil, S., Avci, U., Zhang, T., Cardenas, C. L., & Hahn, M. G. (2015). Immunological approaches to biomass characterization and utilization. *Frontiers in Bioengineering and Biotechnology, 3*, 173.

Pei, Y., Li, Y., Zhang, Y., Yu, C., Fu, T., Zou, J., et al. (2016). G-lignin and hemicellulosic monosaccharides distinctively affect biomass digestibility in rapeseed. *Bioresource Technology, 203*, 325–333.

Peralta, A., Venkatachalam, S., Stone, S., & Pattathil, S. (2017). Xylan epitope profiling: An enhanced approach to study organ development-dependent changes in xylan structure, biosynthesis, and deposition in plant cell walls. *Biotechnology for Biofuels, 10*, 245.

Ragauskas, A. J., Williams, C. K., Davison, B. H., Britovsek, G., Cairney, J., Eckert, C. A., et al. (2006). The path forward for biofuels and biomaterials. *Science, 311*, 484–489.

Scheller, H. V., & Ulvskov, P. (2010). Hemicelluloses. *Annual Review of Plant Biology, 61*, 263–289.

Singh, J., Suhag, M., & Dhaka, A. (2015). Augmented digestion of lignocellulose by steam explosion, acid and alkaline pretreatment methods: A review. *Carbohydrate Polymers, 117*, 624–631.

Somerville, C., Bauer, S., Brininstool, G., Facette, M., Hamann, T., Milne, J., et al. (2004). Toward a systems approach to understanding plant cell walls. *Science, 306*(5705), 2206–2211.

Sun, D., Alam, A., Tu, Y., Zhou, S., Wang, Y., Xia, T., et al. (2017). Steam-exploded biomass saccharification is predominately affected by lignocellulose porosity and largely enhanced by Tween-80 in *Miscanthus*. *Bioresource Technology, 239*, 74–81.

Wang, Y., Huang, J., Li, Y., Xiong, K., Wang, Y., et al. (2015). Ammonium oxalate-extractable uronic acids positively affect biomass enzymatic digestibility by reducing lignocellulose crystallinity in *Miscanthus*. *Bioresource Technology, 196*, 391–398.

Wang, Y., Fan, C., Hu, H., Li, Y., Sun, D., Wang, Y., et al. (2016). Genetic modification of plant cell walls to enhance biomass yield and biofuel production in bioenergy crops. *Biotechnology Advances, 34*(5), 997–1017.

Xie, G., & Peng, L. (2011). Genetic engineering of energy crops: A strategy for biofuel production in China. *Journal of Integrative Plant Biology, 53*(2), 143–150.

Xu, N., Zhang, W., Ren, S., Liu, F., Zhao, C., Liao, H., et al. (2012). Hemicelluloses negatively affect lignocellulose crystallinity for high biomass digestibility under NaOH and H_2SO_4 pretreatments in *Miscanthus*. *Biotechnology for Biofuels, 5*(1), 58.

Zahoor, Sun, D., Li, Y., Wang, J., Tu, Y., Wang, Y., et al. (2017). Biomass saccharification is largely enhanced by altering wall polymer features and reducing silicon accumulation in rice cultivars harvested from nitrogen fertilizer supply. *Bioresource Technology, 243*, 957–965.

Zahoor, Tu, Y., Wang, L., Xia, T., Sun, D., Zhou, S., et al. (2017). Mild chemical pretreatments are sufficient for complete saccharification of steam-exploded residues and high ethanol production in desirable wheat accessions. *Bioresource Technology, 243*, 319–326.

Zhang, W., Yi, Z., Huang, J., Li, F., Hao, B., Li, M., et al. (2013). Three lignocellulose features that distinctively affect biomass enzymatic digestibility under NaOH and H_2SO_4 pretreatments in *Miscanthus*. *Bioresource Technology, 130*, 30–37.

Zhang, M., Wei, F., Guo, K., Hu, Z., Li, Y., Xie, G., et al. (2016). A Novel *FC116/BC10* mutation distinctively causes alteration in the expression of the genes for cell wall polymer synthesis in rice. *Frontiers in Plant Science, 7*, 1366.